Available online at www.sciencedirect.com

SciVerse ScienceDirect

Ceramics International 39 (2013) 1917–1922

CERAMICS INTERNATIONAL

www.elsevier.com/locate/ceramint

Synthesis, luminescence and EPR studies on $CaSiO_3$: Pb, Mn-nano phosphors synthesized by the solution combustion method

Sandhya Kulkarni[a,*], B.M. Nagabhushana[b], N. Suriya murthy[c], C. Shivakumara[d], R.P.S. Chakradhar[e], R. Damle[a,*]

[a]*Department of Physics, Bangalore University, Bangalore 560056, India*
[b]*Department of Chemistry, MSRIT, Bangalore 560012, India*
[c]*Radiological Safety Division, Indira Gandhi Centre for Atomic Research, Kalpakkam 603102, India*
[d]*Department of SSCU, Indian Institute of Science, Bangalore 560012, India.*
[e]*Central Glass and Ceramic Research Institute (CSIR), Kolkata 700031, India*

Received 8 July 2012; received in revised form 14 August 2012; accepted 14 August 2012
Available online 23 August 2012

Abstract

Nano-ceramic phosphor $CaSiO_3$ doped with Pb and Mn was synthesized by the low temperature solution combustion method. The materials were characterized by Powder X-Ray Diffraction (XRD), Thermo–gravimetric and Differential Thermal Analysis (TG–DTA), Scanning Electron Microscopy (SEM) and Transmission Electron Microscopy (TEM). The Electron Paramagnetic Resonance (EPR) spectrum of the investigated sample exhibits a broad resonance signal centered at $g=1.994$. The number of spins participating in resonance (N) and its paramagnetic susceptibility (χ) have been evaluated. Photoluminescence of doped $CaSiO_3$ was investigated when excited by UV radiation of 256 nm. The phosphor exhibits an emission peak at 353 nm in the UV range due to Pb^{2+}. Further, a broad emission peak in the visible range 550–625 nm can be attributed to $^4T_1 \rightarrow {}^6A_1$ transition of Mn^{2+} ions. The investigation reveals that doping perovskite nano-ceramics with transition metal ions leads to excellent phosphor materials for potential applications.

Keywords: Nano-ceramics; Phosphors; Luminescence studies; EPR measurements

1. Introduction

$CaSiO_3$, one of the ceramic materials, is found as a mineral in the lower mantle of the earth. It has a 'distorted cubic' structure. The luminous and electrical properties of the material can be modified by doping impurity atoms viz., rare earth and transition elements. It has excellent chemical stability and thermal stability, and it is one of the promising host luminescent materials [1]. $CaSiO_3$: Pb, Mn is just one kind of photo-luminescent and cathode-ray luminescent phosphors which is widely used due to cheap raw material [2,3]. It is reported in the literature that calcium silicate phosphors activated with varying amounts of manganese, luminesce yellow to orange under cathode-ray excitation. However, it does not exhibit luminescent property when excited by ultraviolet light ($\lambda=253$ nm). If a small amount of lead (Pb) is added with the manganese, the resulting material responds to $\lambda=253$ nm and gives rise to the same color as that produced by cathode-rays in the visible region. In addition to this, it gives rise to an ultraviolet band at $\lambda=340$ nm. The spectral distribution in the visible region is dependent upon manganese concentration and on temperature [4]. Qualitative absorption experiments indicate that the lack of response of $CaSiO_3$: Mn to $\lambda=253$ nm excitation is due to the absence of an absorption for this radiation. Lead (Pb) acts as a sensitizer for manganese by introducing an absorption band in the vicinity of 253 nm. The presence of a sensitizer is unnecessary under cathode ray excitation, since in this case the energy is absorbed by the host crystal itself.

Other than the rare-earth doped phosphors, the manganese ion-doped materials are also good candidates for photonic sources. Many researchers have studied the

---

*Corresponding authors. Tel.: +91 92430 17429.
E-mail address: pappu.sandhyakulkarni@gmail.com (S. Kulkarni).

0272-8842/$ - see front matter
http://dx.doi.org/10.1016/j.ceramint.2012.08.041

luminescence behavior of the Mn^{2+} activators [5–7]. According to reports, the $3d^5$ multiplet energies of Mn^{2+} in crystals depend largely on the co-valency interaction with the host crystal or the crystal field, because the 3d electrons of the transition metal ions are the outermost electrons. The luminescence in Pb, Mn doped lanthanum silicate, was reported by Wanmaker et. al [8]. It was found that fluorescence does not occur by incorporating the activator ions Pb and Mn in the 2:1 compound ($2La_2O_3 \cdot 1SiO_2$). However, the 1:1 compound gives a moderate orange fluorescence while the 1:2 compound exhibits a very weak dark red fluorescence. According to Lingzhun et al. nano-phosphor $CaSiO_3$: Pb, Mn synthesized by the sol–gel method, considering $n(Ca^{2+}):n(Si^{4+})$ ratio as 0.7:1.3 and $Pb^{2+}:Mn^{2+}$ as 0.025:0.033, showed 100% fluorescent intensity [9].

In this present work, we have prepared the $CaSiO_3$: Pb, Mn nano-phosphor by solution combustion method and investigated its luminescence properties. Combustion synthesis is a simple, fast and efficient method for preparing silicate materials [10].

2. Experimental

The $CaSiO_3$ ceramic powder has been prepared by dissolving stoichiometric quantities of Analar grade calcium nitrate ($Ca(NO_3)_2\ 4H_2O$), fumed silica (99.9% pure SiO_2 of surface area 200 m^2/g), and citric acid ($C_6H_8O_7$) (which acts as a fuel for redox reaction) in a minimum quantity of water and dispersed well using magnetic stirrer for half an hour. The heterogeneous redox mixture was rapidly heated in a muffle furnace maintained at 500 ± 10 °C. The redox mixture when heated at 500 °C boils and thermally dehydrates forming a honeycomb like gel, which ignites to yield voluminous $CaSiO_3$ powder. Assuming complete combustion of the mixture used for the synthesis of undoped $CaSiO_3$, the reaction may be written as

$$9Ca(NO_3)_2(aq.) + 9SiO_2(S) + 5C_6H_8O_7(aq.) \rightarrow 9CaSiO_3(S) + 20H_2O(g) + 30CO_2(g) + 9N_2(g) \quad (1)$$

The $CaSiO_3$:Pb, Mn ceramic powder has been prepared by using stoichiometric quantities of calcium nitrate, fumed silica, lead nitrate, manganese nitrate which are in the ratio 0.7:1.3:0.025:0.033 and citric acid in a similar way. The water of hydration of lead and manganese nitrates is neglected, as they are water soluble.

X-ray powder diffractometer (Phillips X'pert) using CuK_α radiation of wavelength 1.540598 Å with a Ni-filter was used to estimate the crystallinity of the phases. The surface morphology and size distribution of the grains were examined by Scanning Electron Microscopy (SEM) and Transmission Electron Microscopy (TEM). Scanning Electron Microscopy was performed with a Philips (XL30-ESEM) instrument. A JEM 2000 Ex instrument was used for Transmission Electron Microscopy. The thermal analysis of the as-formed $CaSiO_3$ powder was carried out using TGA/SDTA 851^e analyzer. The photoluminescence (PL) excitation and emission measurements of doped $CaSiO_3$ were carried out with a Jobin Yvon Spectro-fluorimeter Fluorolog-3 equipped with 450 W Xenonlamp as excitation source. TSL/OSL measurements were carried out with Riso-TL/OSL reader equipped with Sr^{90}/Y^{90} source and optical stimulation was performed by array of blue LEDs.

3. Results and discussions

3.1. Powder X-ray diffraction (PXRD)

Fig. 1 shows the powder XRD pattern of undoped (as-formed and sintered at 500, 700, 800 and 900 °C for 3 h) and Pb, Mn doped $CaSiO_3$ samples. The as-formed powder is amorphous and it remains amorphous until 700 °C after which it gets crystallized at 800 °C. It shows a single β-phase, when sintered at 900 °C for 3 h. The peak positions of β-$CaSiO_3$ phase and their *hkl* values are in good agreement with JCPDS file no. 84-0655. The phase transition temperatures of combustion derived $CaSiO_3$ powder were found to be low compared to the powder obtained in a solid-state reaction method [11]. It is found that, the crystal system of single phase β-$CaSiO_3$ is monoclinic with space group $P2_1/a$. $CaSiO_3$: Pb, Mn powder was also sintered at 900 °C for 3 h and the powder XRD patterns were recorded, which also shows the β-phase with no change in the structure. This confirms that Pb^{2+} and Mn^{2+} occupy the Ca^{2+} sites. It is reported by Liangzhun et al. that $CaSiO_3$ synthesized by the sol–gel method shows β-phase, when sintered at 900 °C for 2 h. However, it shows a mixed phase when sintered at higher temperatures [9].

The crystallite size of the ceramic powders is calculated from the full width at half maximum (FWHM) of the diffraction peak of the powders from line broadening Scherrer's formula $D = k\lambda/(\mathrm{FWHM}\cos\theta)$, where λ is the wavelength of X-ray, θ the Bragg angle and k is a constant which depends on the grain shape (0.89 Å for circular

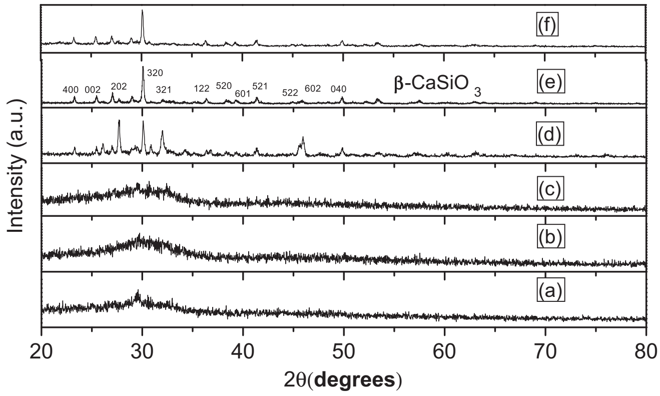

Fig. 1. Powder XRD patterns of $CaSiO_3$ (a) as formed, (b) 500 °C (3 h), (c) 700 °C (3 h), (d) 800 °C (3 h), (e) 900 °C (3 h), and (f) $CaSiO_3$: Pb, Mn sintered at 900 °C for 3 h.

grains). It was observed that the average crystallite size of β-$CaSiO_3$ samples lie in the range of 20–30 nm.

3.2. TG–DTA measurements

The thermal decomposition behavior of the $CaSiO_3$ sample has been studied by TG–DTA. The TGA and DTA thermograms are shown in Fig. 2. The big endothermic peak at 210 °C can be attributed to the evaporation of residual water and nitrate content in the sample. The TG curve shows about 2.0% weight loss from room temperature 37 °C to 515 °C corresponding to the endothermic DTA peak. Another endothermic observed at 619 °C with weight loss may be related to the elimination of the organic compounds chemically bound to Ca and Si. The small exothermic effect at 841 °C can be attributed to the crystallization of $CaSiO_3$ and a small hump (exothermic effect) at 920 °C represents a phase transformation into β-$CaSiO_3$ host lattice in confirmation with XRD results. The TG curve shows no obvious weight change when the temperature is higher than 800 °C, and the corresponding small exothermic curve in DTA is due to the gradual formation of β-$CaSiO_3$ crystalline phase confirmed by XRD.

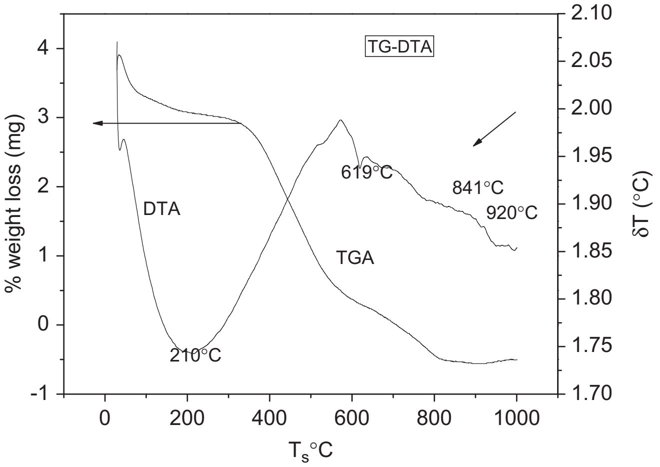

Fig. 2. TG–DTA thermograms of β-$CaSiO_3$.

3.3. Scanning Electron Microscopy (SEM) and Transmission Electron Microscopy (TEM)

The morphology and size distribution of doped and undoped samples were examined using scanning electronic microscopy and the images are depicted in Fig. 3. It is interesting to note that β-$CaSiO_3$ is porous and the particles are agglomerated. The particle agglomeration is retained in the β-$CaSiO_3$ doped with Pb^{+2} and Mn^{+2} and the morphology of the doped sample is different from that of the undoped sample. The liberation of gaseous products during combustion reaction increases the surface area of the powder product by creating micro and nano-porous regions, as shown in the SEM photographs.

TEM image of $CaSiO_3$: Pb, Mn shown in Fig. 4. It is seen that the crystallites are irregular in shape and size and are agglomerated. The size of the agglomerated crystallites is found to be about 200 nm.

3.4. Photoluminescence studies

The excitation spectrum for $CaSiO_3$: Pb, Mn shows a dominant peak at 256 nm (peak (a) in Fig. 5). It gives rise to an emission band observed at 353 nm (peak (c)). This broad peak perhaps originates from $^3P_1 \rightarrow {}^1S_0$ optical transition of Pb^{+2}. The co-doping of $CaSiO_3$: Pb with divalent Mn gives interesting results. Upon excitation at 256 nm, we observe an emission at 353 nm due to Pb^{2+} and another emission from Mn^{2+} at 590 nm as shown in Fig. 6. This near red emission in the visible region is due to transition from $^4T_0$ to $^6A_1$ level of Mn^{2+}. The excitation wavelength of $CaSiO_3$ doped with only Mn^{2+} is 354 nm [12] whereas the characteristic emission wavelength of the Pb^{2+} doped system is found to be 353 nm. This shows a significant overlapping of emission maxima of donor and excitation maxima of acceptor leading to energy transfer from Pb^{2+} to Mn^{2+}. This is further confirmed by the observation of donor absorption band at 257 nm (peak (b) in Fig. 5). Such sensitization has been reported in other silicates hosts too [13]. Fig. 7 represents the energy level diagram showing the energy transfer from Pb^{2+} to Mn^{2+}.

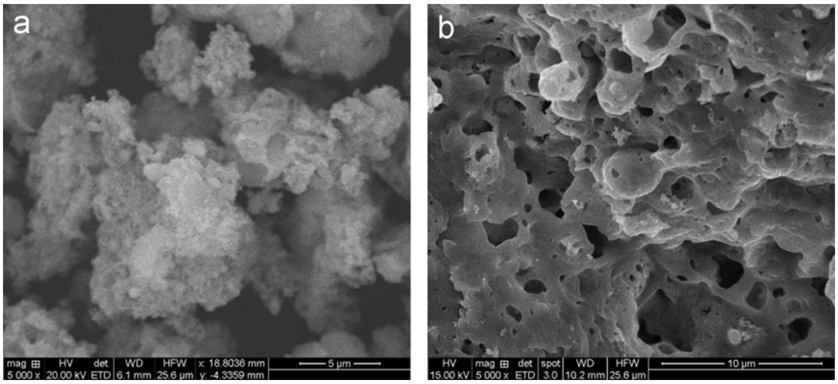

Fig. 3. SEM images of (a) β-$CaSiO_3$ and (b) $CaSiO_3$: Pb, Mn.

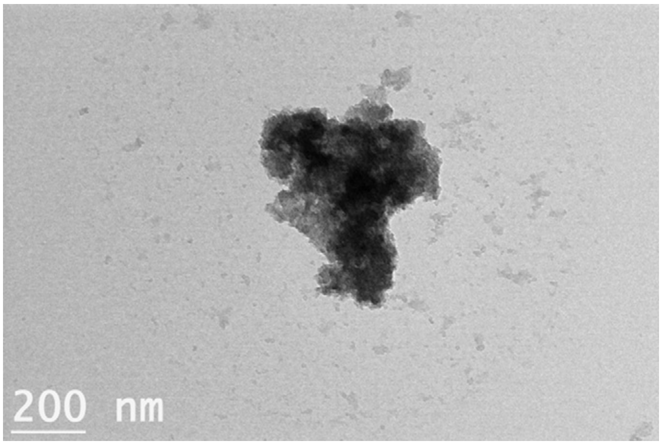

Fig. 4. TEM image of $CaSiO_3$: Pb, Mn.

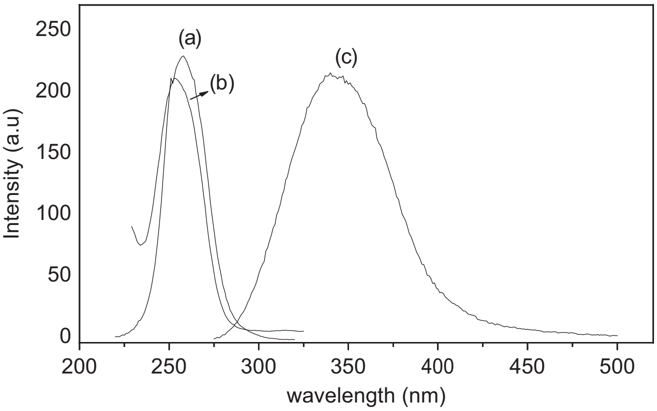

Fig. 5. (a) Excitation peak of Pb^{+2} in $CaSiO_3$:Pb, Mn (b); excitation peak of Mn^{+2} in $CaSiO_3$:Pb, Mn; and (c) emission spectra of Pb^{+2} in $CaSiO_3$:Pb, Mn.

The strong orange to red emission in the region 550–625 nm in $CaSiO_3$: Pb, Mn phosphor is due to the relaxation of the electrons in the conduction band to the $^4T_1$ excited state by non radiative process followed by radiative transition from the excited state $^4T_1$ to $^6A_1$ ground state. It has been reported in literature that the tetrahedrally coordinated Mn^{2+} ions give a green emission, whereas octahedrally coordinated Mn^{2+} ions give an orange to red emission [14]. In the present work, we have observed orange to red emission peak around 550–625 nm in photoluminescence studies which confirms that the Mn^{2+} ions possess octahedral symmetry.

3.5. Thermoluminescence studies

Thermo stimulated luminescence (TSL) spectrum of $CaSiO_3$: Pb, Mn recorded after exposure to 1 mGy ^{60}Co gamma dose is depicted in Fig. 8(a). The appearance of single glow peak in TSL glow curve appearing at 157 °C obviously indicates the presence of only one trap which is responsible for thermo-luminescence emission. Gamma irradiated phosphor exhibits optically stimulated luminescence (OSL) presented in Fig. 8(b). This was recorded in continuous mode (CM-OSL) wherein optically stimulated traps were emptied upon irradiation by blue LEDs.

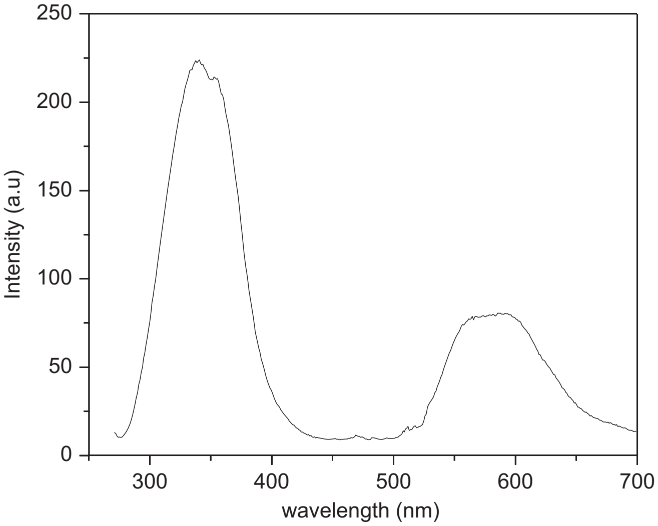

Fig. 6. Emission spectra of $CaSiO_3$: Pb, Mn when excited at 256 nm.

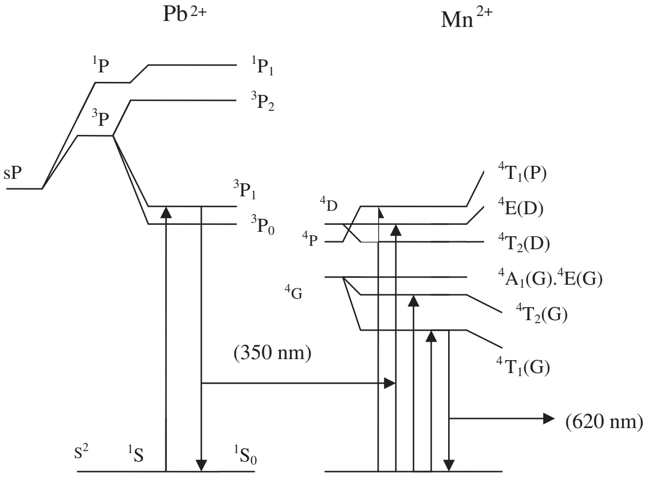

Fig. 7. Energy level diagram depicting energy transfer from Pb^{2+} to Mn^{2+}.

3.6. Electron Paramagnetic Resonance (EPR) studies

Fig. 9 shows the EPR spectrum of $CaSiO_3$: Pb, Mn phosphor at room temperature. The EPR spectrum of the investigated sample exhibit a broad resonance signal centered at $g \approx 1.994$ due to Mn^{2+} ($3d^5$: $^6S_{5/2}$) ions entering the matrix as paramagnetic species. In case of d^5 transition metal ions, it is known that axial distortion of octahedral symmetry gives rise to three Kramers doublets $|\pm 5/2>$, $|\pm 3/2>$ and $|\pm 1/2>$ [15]. Application of a Zeeman field lifts the spin degeneracy of Kramer's doublets. As the crystal field splitting is normally much greater than the Zeeman field, the resonances observed are due to

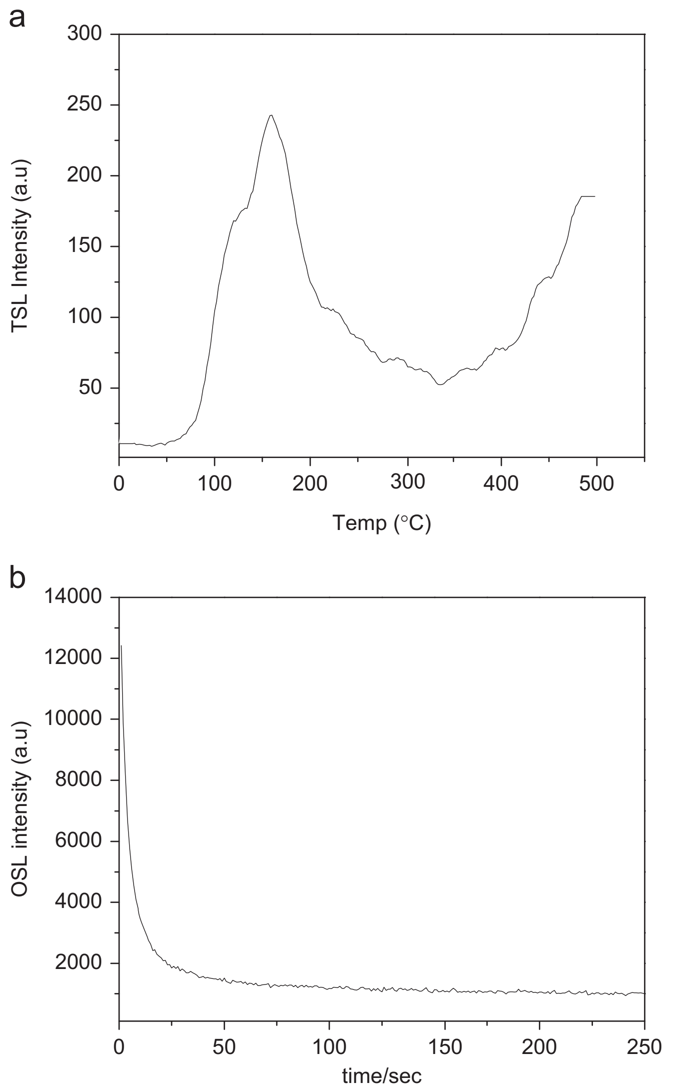

Fig. 8. (a) Thermoluminescence glow curve of $CaSiO_3$: Pb, Mn (b) OSL (continuous mode) decay curve of $CaSiO_3$: Pb, Mn.

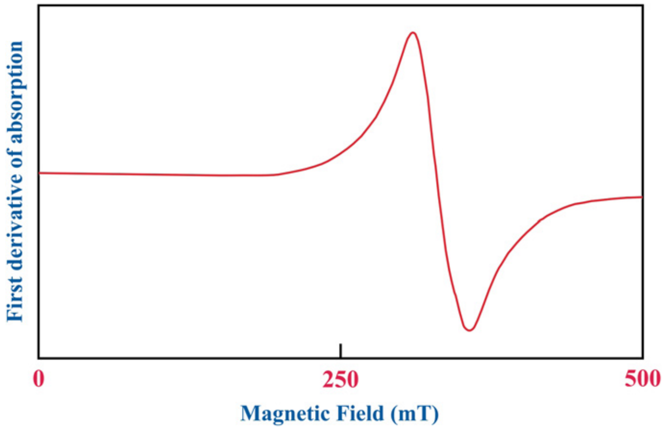

Fig. 9. EPR spectrum of $CaSiO_3$: Pb, Mn.

transitions within the Zeeman field split Kramers doublets. The resonance at $g \approx 2.0$ is due to the Mn^{2+} ions in an environment close to octahedral symmetry and is known to arise from the transition between the energy levels of the lower doublet.

The spin concentration (N) participating in resonance can be calculated by comparing the area under the absorption EPR signal with that of a standard ($CuSO_4 \cdot 5H_2O$ in this study) of known concentration. The expression for the spin concentration which includes the experimental parameters of both sample and the standard, as given by Weil et al. [16] is

$$N = \frac{A_x(Scan_x)^2 G_{std}(B_m)_{std}(g_{std})^2[S(S+1)]_{std}(P_{std})^{1/2}}{A_{std}(Scan_{std})^2 G_x(B_m)_x(g_x)^2[S(S+1)]_x(P_x)^{1/2}[Std]} \qquad (2)$$

where A is the area under the absorption curve which can be obtained by double integrating the first derivative EPR absorption curve, scan is the magnetic field corresponding to unit length of the chart, G is the gain, B_m is the modulation field width, g is the g-factor, S is the spin of the system in its ground state and P is the power of the microwave. The subscripts 'x' and 'Std' represent the corresponding quantities for Mn^{2+} in $CaSiO_3$: Pb, Mn phosphor and the reference $CuSO4 \cdot 5H_2O$ respectively. The spin concentration evaluated using the above equation is $N = 2.94 \times 10^{18}$.

The EPR data can be used to calculate the paramagnetic susceptibility χ [17] of the sample using the formula

$$\chi = \frac{Ng^2\beta^2 J(J+1)}{3k_B T} \qquad (3)$$

where N is the number of spins per m^3 and the other symbols have their usual meaning. The paramagnetic susceptibility evaluated from EPR data for $CaSiO_3$: Pb, Mn phosphor is $7.128 \times 10^{-7}\ m^3\ kg^{-1}$.

4. Conclusions

The powder XRD confirms that the synthesized material $CaSiO_3$ is in β-phase. The powder diffractogram of the Pb and Mn doped $CaSiO_3$ are unaltered indicating that the Pb^{2+} and Mn^{2+} occupy the Ca^{2+} site. Photoluminescence measurements under UV excitation at 256 nm exhibit an emission band at 353 nm in the UV region originating from $^3P_1 \rightarrow {}^1S_0$ optical transition of Pb^{2+}. The codoping of $CaSiO_3$: Pb with Mn results in an emission band around 590 nm due to energy transfer from Pb^{2+} to Mn^{2+}. Pb^{2+} thus acts as a sensitizer. The material gives rise to a TSL glow curve at 157 °C after exposure to gamma radiation. The observed EPR signal corresponding to $g \approx 2$ indicate the presence of manganese ions in an environment close to octahedral symmetry.

Acknowledgment

The author Sandhya Kulkarni wishes to acknowledge the University Grants Commission (UGC), Government of India, for the award of UGC-FIP fellowship to carry out this work.

References

[1] Liu Xingren, Zhang Xiao, Lu Shuhua, Zhang Yinglan, Luminescence properties of Ce^{3+} in calcium metasilicate, Chinese Journal of Luminescence 10 (3) (1989) 177–185.

[2] J.R. Qiu, N. Sugimoto, Y. lwabuehi, K. Hirao, Photostimulated luminescence in Ce^{3+}-doped silicate glasses, Journal of Non-Crystalline Solids 209 (1997) 200–203.

[3] T.J. Glynn, N.V. Kuleshov, V.P. Mikhailov, V.G. Scherbitsky, B.I. Minkov, R. Sherlock, Luminescence study of Cr^{4+}-doped silicates, Optical Materials 4 (1995) 507–513.

[4] Frank J. Studer, Gorton R. Fonda, Optical properties of $CaSiO_3$, Journal of the Optical Society of America 39 (8) (1949) 655–660.

[5] C.R. Ronda, T. Amrein, Evidence for exchange induced luminescence in Zn_2SiO_4, Journal of Luminescence 69 (1996) 245.

[6] D.T. Palumbo, J.J. Brown Jr., Electronic states of Mn^{2+}-activated phosphors, Journal of the Electrochemical Society 117 (1970) 1184.

[7] L.E. Shea, R.K. Datta, J.J. Brown Jr., Low voltage cathodoluminescence of Mn^{2+}-activated $ZnGa_2O_4$, Journal of the Electrochemical Society 141 (1994) 1950.

[8] W.L. Wanmaker, W.P. De Graaf, H.L. Spier, Luminescence of Pb and Pb–Mn-activated lanthanum silicates 25 (1959) 1125–1130 Physica 25 (1959) 1125–1130.

[9] Yang Liangzhun, Fang Min, Liu Yuejiao, Liu Chao, Wang Xiuying, Y.U. Xibin, Preparation and properties of luminous materials of $CaSiO_3$: Pb, Mn by sol–gel method, Frontiers of Chemistry in China 2 (4) (2007) 442–446.

[10] V.B. Bhatkar, S.K. Omanwar, S.V. Moharil, Combustion synthesis of silicate phosphors, Optical Materials 29 (2007) 1066–1070.

[11] B.M. Nagabhushana, R.P.S. Chakradhar, K.P. Ramesh, V. Prasad, C. Shivakumara, Effect of fuel on the formation structure, transport and magnetic properties of $LaMnO_3$ nanopowders, Philosophical Magazine 90 (2010) 2009–2025.

[12] Shi Ye, Xiao-Ming Wang, Xi-Ping Jing, Energy transfer among Ce^{3+}, Eu^{2+} and Mn^{2+} in $CaSiO_3$, Journal of the Electrochemical Society 155 (6) (2008) J143–J147.

[13] T.H.P.J. Botden, F.A. Kroger, Energy transfer in sensitized $Ca_3(PO_4)_2$-Ce–Mn and $CaSiO_3$–Pb–Mn, Physica XIV 8 (1948) 553–566.

[14] G. Blasse, B.C. Grabmaier, Luminescent Materials, Springer-Verlag, Berlin, 1994.

[15] A. Abragam, B. Bleaney, Electron Paramagnetic Resonance of Transition Ions, Clarendon, Oxford, 1970.

[16] J.A. Weil, J.R. Bolton, J.E. Wertz, Electron Paramagnetic Resonance—Elementary Theory and Practical Applications, Wiley, Newyork, 1994, p. 498.

[17] N.W. Ascheroft, N.D. Mermin, Solid State Physics, Harcourt College Publishers, 2001, p. 656.